

Damping of Surface Pressure Fluctuations in Hypersonic Turbulent Flow Past Expansion Corners

Kung-Ming Chung* and Frank K. Lu†

University of Texas at Arlington, Arlington, Texas 76019

Surface pressure fluctuations of Mach 8 turbulent flow past a 2.5- and a 4.25-deg expansion corner maintained a Gaussian distribution but were severely attenuated by the expansion process. The pressure fluctuations did not recover to those of an equilibrium turbulent flow even though the mean pressures reached downstream inviscid values in four to six boundary-layer thicknesses. The fluctuations were convected with a velocity comparable to that on a flat plate, and they maintained their identities longer for the stronger expansion. The damping of pressure fluctuations at hypersonic Mach numbers, even by small corner angles, may be exploited in fatigue design.

Nomenclature

| | |
|---------------------|---|
| \bar{D}_c | = normalized convection distance, $\tau U_c / \delta_0$ |
| f | = frequency |
| K | = hypersonic similarity parameter, $M_\infty \alpha$ |
| M | = Mach number |
| p | = pressure |
| q | = dynamic pressure |
| $R_{pp}(\xi, \tau)$ | = normalized wall pressure space-time correlation between transducers 1 and 2, $[(1/N) \sum_{n=1}^N p_1(t_n) p_2(t_n + \tau)] / [\sigma_{p_1} \sigma_{p_2}]$ |
| Re | = unit Reynolds number |
| T | = temperature |
| U | = velocity |
| U_τ | = friction velocity, $\sqrt{\tau_w / \rho_w}$ |
| x | = coordinate along the surface of the corner, see inset to Fig. 2 |
| \bar{x} | = x / δ_0 |
| α | = expansion corner angle |
| δ | = boundary-layer thickness |
| ν | = kinematic viscosity |
| ξ | = transducer spacing |
| σ_p | = standard deviation of surface pressure fluctuations, $\{\sum_{n=1}^N [p(t_n) - \langle p \rangle]^2 / N\}^{1/2}$ |
| τ | = wall shear stress or time delay in autocorrelations and cross correlations |
| $(-)$ | = normalized by undisturbed boundary-layer thickness at the corner |
| $(-)'$ | = fluctuating component of surface pressure |

Subscripts

| | |
|----------|---|
| c | = convective |
| o | = stagnation condition |
| w | = wall |
| 0 | = undisturbed conditions at the corner location |
| ∞ | = incoming freestream |

Introduction

THERE has recently been some interest in the supersonic turbulent flow past an expansion corner primarily in examining the effect of expansion on the turbulence structure.^{1,2}

Received April 17, 1992; revision received Nov. 4, 1992; accepted for publication Nov. 9, 1992. Copyright © 1993 by K.-M. Chung and F. K. Lu. Published by the American Institute of Aeronautics and Astronautics, Inc., with permission.

*Graduate Research Associate, Aerodynamics Research Center, Mechanical and Aerospace Engineering Department. Student Member AIAA.

†Assistant Professor, Aerodynamics Research Center, Mechanical and Aerospace Engineering Department. Senior Member AIAA.

These studies applied rapid distortion approximations to predict the Reynolds stresses with good accuracy. Both experiment and analysis show dramatic decreases in velocity fluctuations and Reynolds stresses but not of the mass-flux fluctuations.² Further, mean velocity profiles^{1,3,4} show tremendous amounts of distortion of the outer layer from the fully developed, equilibrium, turbulent profile. In addition, in some instances a "sub-boundary layer" develops through a thickening of the viscous sublayer that indicates that the boundary layer may "relaminarize,"⁵ a term that should however be used with caution in view of the nearly unattenuated mass-flux fluctuations downstream.²

Most recently, the mean surface pressure distribution has been studied to identify parameters that govern the expansion process.⁶ The study found that the surface pressure asymptotically approaches the downstream inviscid pressure, but for practical purposes a downstream influence can be identified. This downstream influence, normalized by the corner boundary-layer thickness, scales to first order with a hypersonic similarity parameter⁷

$$K = M_\infty \alpha \quad (1)$$

The aforementioned studies have contributed to the understanding of a number of key mean and fluctuating features. Nonetheless, the effect of the expansion on surface pressure fluctuations has not been studied at all to the authors' knowledge. Surface pressure fluctuations are an important aspect of turbulent flows and their accurate knowledge is crucial in structural design. The knowledge is especially necessary at hypersonic Mach numbers because the rms value of the fluctuations is proportional to M^2 for turbulent flows past cold walls.⁸ This paper intends to fill gaps in the state of understanding by reporting an experimental study aimed at examining the effect of an expansion corner on the surface pressure fluctuations of an incoming hypersonic turbulent flow. Before discussing the data, the experimental techniques used are briefly described.

Experimental Techniques

Test Facility and Models

The experiments were performed in the University of Texas at Arlington's hypersonic shock tunnel facility. The shock tunnel and its operation were previously reported,^{6,9} and only a brief description is provided here. The shock tunnel was operated in the reflected, equilibrium interface mode.¹⁰ A double-diaphragm section was used to separate the driver and driven gases and to obtain precise control of the driven- and driver-tube pressures and the tunnel firing sequence that, in turn, allowed accurate control of stagnation conditions and

unit Reynolds number. The test gas, which was dried air, was expanded by a conical nozzle with a 7.5-deg half-angle connected to a semifree jet test section 536 mm (21.1 in.) long and 440 mm (17.5 in.) in diameter.

A stainless steel flat plate 203 mm (8 in.) wide by 0.96 m (37.75 in.) long with a sharp convex corner located at 768 mm (30.25 in.) from its leading edge was used to develop a boundary layer. The flat plate had a 15-deg sharp leading edge and was mounted 50 mm (2 in.) below the tunnel centerline to avoid "wave focusing" along the centerline in axisymmetric test sections.¹¹ Further, side plates were attached along both bottom edges of the flat plate to prevent crossflows.¹² Two models were tested, and they had corner angles of $\alpha = 2.5$ and 4.25 deg, respectively, both accurate to ± 0.1 deg. The angles were chosen so that the values of K of 0.35 and 0.59 were comparable with those of earlier studies.^{1-4,6,13,14} In the test region, starting at about 750 mm (29.5 in.) from the flat-plate leading edge, the surface pressures without the corner showed an extremely slight, favorable longitudinal pressure gradient that can be ignored. Within experimental accuracy, the undisturbed surface pressures were assumed uniform. Pressure taps for flush-mounted transducers were drilled perpendicularly onto the test surface from 38.1 mm (1.5 in.) upstream to 60.3 mm (2.375 in.) downstream of the corner location. The taps were offset from the centerline by 3.18 mm (0.125 in.) and were spaced 6.35 mm (0.25 in.) or $0.47\delta_0$ apart.

Test Conditions

The tunnel was operated by first charging the driver tube and the double-diaphragm section to 24 MPa $\pm 1.5\%$ (3500 psia) and 12 MPa (1750 psia), respectively. Room air was evacuated from the driven tube that was then charged with dried air to 280 kPa $\pm 1.3\%$ (40 psia), whereas the test section, diffuser, and dump tank were evacuated to less than 0.32 kPa (0.05 psia). The tunnel was started by breaking the two diaphragms through venting the double-diaphragm section. A shock propagated into the driven tube and an unsteady expansion propagated into the driver tube. The speed of the shock was determined by timing the shock passage at two locations toward the end of the driven tube using flush-mounted pressure transducers. A shock Mach number of 2.15 with a run-to-run variation of less than $\pm 5\%$ was obtained. The low value of the shock Mach number insured that real gas effects were negligibly small. The test conditions obtained are displayed in Table 1. The poor estimate of the shock Mach number was due to difficulty in resolving the shock fronts and was not due to poor control of the initial tunnel conditions. The stagnation pressure and temperature and the unit Reynolds number were sensitive to the estimate of shock Mach number. The 5% resolution in estimating the shock Mach number resulted in an estimated maximum scatter of 13, 7, and 20% for the three respective properties. The run-to-run variation in measured pressure was minimized by normalizing the measurements with a mean reference pressure. The downstream inviscid conditions for the 2.5- and 4.25-deg corners were static pressures and temperatures of 0.33 kPa (0.048 psia) and 51 K (92°R) and 0.23 kPa (0.033 psia) and 46 K (83°R), respectively. These conditions were close to but above the air saturation line.¹⁵ The respective downstream Mach numbers were 8.65 and 9.15. The flat plate was at room temperature ($T_w \approx 290$ K, 522°R), and thus the experiments were performed under cold-wall conditions ($T_w/T_o \approx 0.35$). Finally, the undisturbed boundary layer developed naturally on the flat plate. In the test region, the undisturbed boundary layer possessed features typical of a low Reynolds number, turbulent flow with a negligible wake component.¹⁶ The boundary-layer thickness at the corner location was estimated to be 13.5 ± 2 mm (0.53 ± 0.08 in.), whereas $Re_\theta = 1.8\text{--}2.3 \times 10^3$ throughout the measurement region.^{17,18} To illustrate the preceding observations, the flat-plate velocity profiles through the test region subjected to the van Driest II transformation¹⁹ and plotted in wall coordinates are shown in Fig. 1. Also shown is a combined wall-wake law fitting the data.²⁰

A test flow of about 0.5-ms duration was established at the interaction region after a starting time of about 2 ms. The test time corresponded to a slug of test gas 0.6 m long. The interaction region along the expansion corner of about 0.2 m or one-third the length of test gas more than fulfilled the requirement for a fully developed turbulent flow to exist.²¹ Further, it can be noted here that the test times provided the lower cutoff frequency to the test data, this frequency being about 2 kHz.

Data Acquisition

Kulite Model XCS-093-5A and XCS-093-50A transducers with 0–35 kPa (0–5 psia) and 0–350 kPa (0–50 psia) ranges having Type "M" protective screens and sensing surfaces of 0.97 mm (0.038 in.) diameter were used. The transducers were potted in place using silicone rubber sealant, and the flushness of the transducers, important in dynamic measurements, had a tolerance of better than $0.005\delta_0$. Only eight data-acquisition channels were available; thus, the surface pressure distribution was built up from a number of runs. Seven channels were used to obtain the pressure distribution, whereas the eighth was used to measure the reference pressure p_∞ at 34.9 mm (1.375 in. or $2.59\delta_0$) ahead of the corner. Unused orifices were plugged with dummy transducer replicas made from steel rods.

According to the manufacturer, the -5 and -50 A transducers had natural frequencies of 100 and 200 kHz, respectively. Moreover, the eight surface pressure signals were conditioned by instrumentation amplifier filters with 100-kHz bandwidths and gains of 500 and were acquired simultaneously at a rate of one million samples per second per channel. Thus, the bandwidth of the data was about 2–100 kHz. After filtering, the signal-to-noise ratio of the measurements was better than 10:1. It was further estimated that about 60% of the rms fluctuations were captured within the data bandwidth.²² The Kulite transducers were calibrated in situ against an MKS Baratron Model 127A vacuum gauge, a capacitance-type manometer accurate to ± 7 Pa (± 0.001 psia), before a daily set of runs. The calibrations were checked continually throughout the daily test sequence, and the transducers were recalibrated if necessary to minimize drift.²³ In the data reduction, the mean surface pressures were adjusted for drift.⁹

Each data record possessed about 500 data points that were deemed adequate for statistical analyses. To check if the earlier statement is valid, a number of data records were divided into two halves, and the mean and rms values of these halves were compared. The mean and rms values differed from 1 to 12% and differed by 6% on average. Therefore, it was thought that the amount of data per record was sufficient.

In analyzing the data, the transducer spatial and frequency resolution limits were considered. The 100-kHz transducer bandwidth severely limited the upper nondimensional fre-

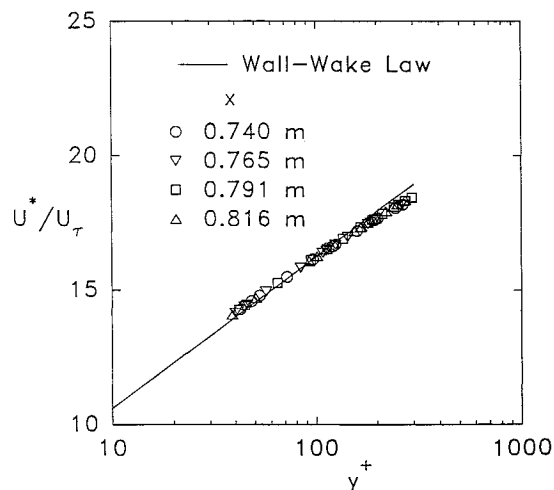


Fig. 1 Transformed velocity profiles in wall coordinates.

quency $f\delta/U_\infty$ to about 1.0, which was low compared with previous dynamic measurements.²⁴ The frequency resolution was also compared with those of different investigations by using a reduced frequency $f\nu_w/U_\tau^2$. In the present experiments, $f\nu_w/U_\tau^2 \approx 0.008$, which was also comparatively low.²⁴ In addition to the bandwidth limitation, high-frequency damping was also partly due to transducer size. A nondimensional transducer diameter $d^+ = U_\tau d/\nu_w$ was used for examining the effects of transducer size on spatial resolution, d being the transducer diameter. In the present experiments, $d^+ \approx 200$, which was in the 50–500 range of most supersonic experiments.²⁴ It remained unclear how d^+ , $f\delta/U_\infty$, or $f\nu_w/U_\tau^2$ could be used to provide proper estimates of transducer spatial and frequency resolutions at high Mach numbers. The inability to resolve the highest frequencies means that knowledge of the spectral behavior of the finest scales that adjusts rapidly downstream of the corner was missing. Finally, it may also be noted that no corrections were made to the data due to the transducer size.

Results and Discussion

The mean surface pressure distributions for the two test cases are plotted in Fig. 2. The pressure distributions approached the downstream inviscid values some distance from the corner. To quantify this strictly asymptotic pressure decay, a downstream influence of the corner can be defined as the intersection of the tangent through the downstream pressure data with the inviscid downstream pressure.⁶ The downstream influence was found to scale with the hypersonic similarity parameter K for a wide range of Mach numbers. The pressure fluctuations remained Gaussian downstream of the expansion corner as is illustrated in Fig. 3, which plots the normalized probability density function (PDF) against the standard deviation

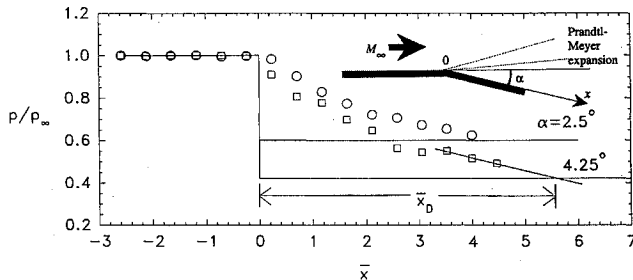


Fig. 2 Surface pressure distribution of turbulent flow past 2.5- and 4.25-deg expansion corners at Mach 8.

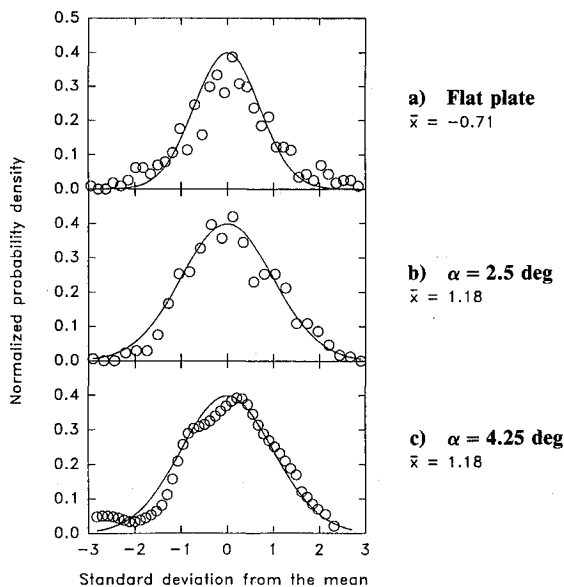


Fig. 3 PDFs of surface pressure fluctuations.

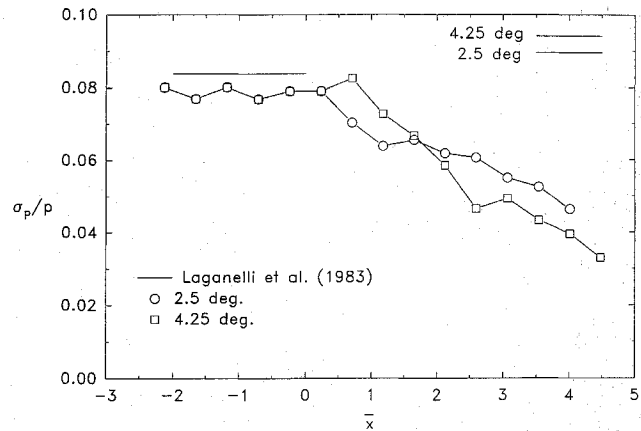


Fig. 4 Standard deviation of surface pressure fluctuations past expansion corners normalized by local mean pressure.

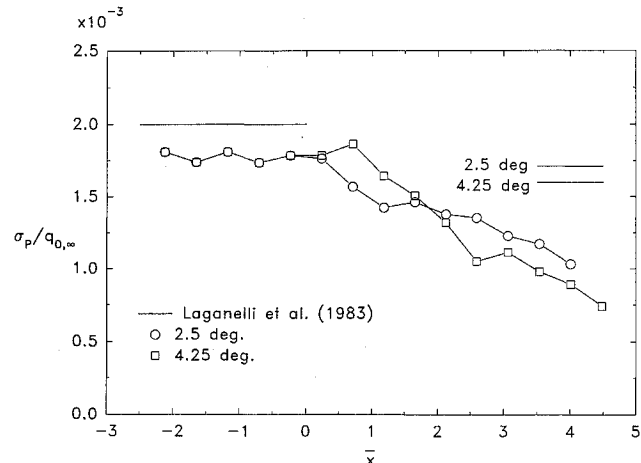


Fig. 5 Standard deviation of surface pressure fluctuations past expansion corners normalized by incoming freestream dynamic pressure.

tion from the mean²⁵ for an undisturbed location at $\bar{x} = -0.71$ and for downstream locations at $\bar{x} = 1.18$. The PDF of the 4.25-deg expansion showed more distortion from the Gaussian than that of the 2.5-deg expansion. This might be due to an insufficiently long data record because contamination from the tunnel starting and stopping processes gave rise to slightly higher pressures at both ends of the data record, thereby causing the PDF to be skewed slightly.

The standard deviations of the surface pressure fluctuations were normalized by the local mean surface pressure, by the dynamic freestream pressure at $\bar{x} = 0$, and by the incoming standard deviation and are plotted in Figs. 4–6, respectively. Moreover, the ensemble of all of the upstream transducers yielded σ_p values that differed by about 2% and this was presumed to be the error in the σ_p estimate through the expansion downstream. Plotted in Fig. 4 is Laganelli et al.'s⁸ semi-empirical correlation for a flat-plate boundary layer for $\bar{x} < 0$. It can be seen that the measured upstream surface pressure fluctuations were slightly below but probably within the range of validity of that predicted by Laganelli et al. The lower fluctuation level measured might be due to the limited frequency bandwidth of the present experiments. Nonetheless, the discrepancy between the present data and Laganelli et al.'s prediction was not severe.

In addition, the data showed the intuitive expectation of a decrease in the fluctuations downstream of the expansion corner, with σ_p/p decreasing from about 0.08 upstream to about 0.046 and about 0.033 for $\alpha = 2.5$ and 4.25 deg, respectively, at $\bar{x} = 4$. Similarly, $\sigma_p/q_{0,\infty}$ decreased from about 0.002 on the flat plate to about 0.001 and about 0.0007 for the two respective corners at $\bar{x} = 4$ (Fig. 5). Moreover, the σ_p data did

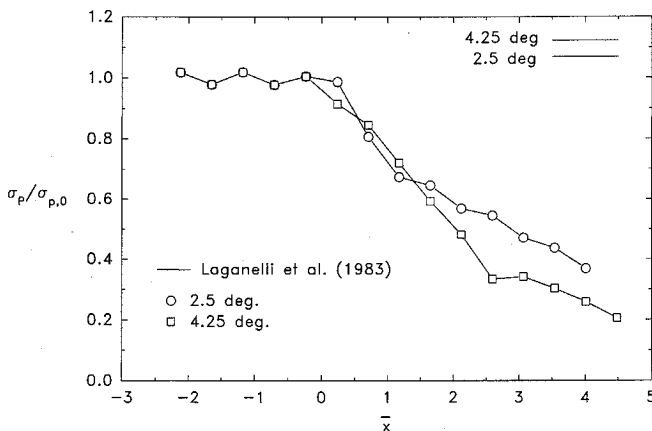


Fig. 6 Standard deviation of surface pressure fluctuations past expansion corners normalized by incoming value.

not show any asymptotic behavior or an increase within the measurement range that might indicate either formation of a new "quiescent" sub-boundary layer or retransition to a fully developed turbulent flow. The data indicated that the effect of the expansion process on the surface pressure fluctuations was incomplete even at the most downstream measurement station and, most likely, that the boundary layer was in nonequilibrium. Further, using the predictions of Laganelli et al.,⁸ the downstream pressure fluctuations for a fully developed, turbulent, flat-plate flow were estimated and are shown as short horizontal lines at the right in Figs. 4–6. It can be seen in Fig. 4 that, at the most downstream measurement station, σ_p/p was about 45 and 60% below the turbulence predictions for the two respective weaker and stronger expansions. In terms of dynamic pressure, the surface pressure fluctuations were about 40% below the turbulence predictions for the 2.5-deg corner and were about 53% below the predictions for the 4.25-deg corner (Fig. 5). It is obvious that the surface pressure fluctuations for the stronger expansion would take a longer distance to recover to the presumably ultimate turbulent level given a sufficiently long downstream length.

Another way of viewing the surface pressure fluctuation development is to compare the fluctuations with that of the incoming boundary layer, as shown in Fig. 6. Figure 6 emphasizes even more clearly the attenuation provoked by the favorable pressure gradient. It can be seen that the surface pressure fluctuations four boundary-layer thicknesses downstream of the corner damped to only 37 and 21% of the incoming value for the 2.5- and 4.25-deg corners, respectively. Possibly, these downstream fluctuation levels could be the "tare" levels of the shock tunnel, although this was expected to be unlikely since the tunnel vibrations were at lower frequencies. The data indicated once again that the flow at four to five boundary-layer thicknesses downstream of the corner was still relatively quiescent. Although data are unavailable currently and are probably unfeasible to obtain, it is thought that the boundary layer would revert to an equilibrium turbulent state based on low-speed observations and that the entire "recovery" process would occupy a long distance of possibly hundreds of boundary-layer thicknesses downstream of the corner.²⁶ This behavior can be significant in the design of high-speed vehicles where even relatively weak expansions such as used in the present study can be used to severely attenuate surface pressure fluctuations, perhaps for considerable distances downstream.

It is also interesting to examine the space-time cross correlation of the surface pressure fluctuations. Three space-time correlations are plotted in Figs. 7a–7c, namely those of a flat plate and the two expansion corners, for comparison. That of the flat plate was obtained upstream of the corner for transducer spacings of $\xi = 0.47$ and 0.94 , whereas those of the expansions were obtained with the first transducer located at

$\bar{x} = 1.18\delta_0$ and with two additional transducers downstream spaced at $0.47\delta_0$ intervals. The cross correlations downstream of the expansion appeared broadly similar in shape as that of the flat plate. These cross correlations were also typical of turbulent flows in which the maxima occur at a positive time delay τ^* . A convection velocity can therefore be defined as

$$U_c \equiv \xi/\tau^* \quad (2)$$

The convective velocity suggests that a disturbance, in this case a wall pressure signal, is convected from one transducer to a downstream transducer at a time interval τ^* . The actual estimates of U_c are, however, prone to error due to difficulties in resolving the maxima accurately. In the present data, a $1\text{-}\mu\text{s}$ error resulted in an error of 10% to U_c , and similar error bands can be inferred from previous investigations.²⁴ Within the accuracy of the present measurements, the convection velocity for a given transducer was roughly constant regardless of the test configuration. Thus, for a transducer spacing of $\xi = 0.47\delta_0$, $U_c/U_\infty = 0.65, 0.71$, and 0.55 for the flat plate and for the 2.5- and 4.25-deg corner, respectively, where U_∞ is the incoming freestream velocity. Further, for a transducer spacing of $\xi = 0.94\delta_0$, $U_c/U_\infty = 0.70, 0.79$, and 0.60 for the three configurations, respectively. There appeared to be a definite trend of an increase of U_c with ξ , this being also observed by previous investigators for flat-plate flows.²⁴ The increase in convection velocity is commonly interpreted as follows. Small-scale (or high-frequency) components of the pressure fluctuations are thought to travel downstream slowly since these fluctuations, being small, would be convected at velocities more typical of the lower portion of the boundary layer. These small fluctuations also have a short "time constant" and decay rapidly. On the other hand, the large-scale pressure fluctuations can be expected to be associated with large eddies within the boundary layer that are convected downstream at higher velocities.

The individual transducer data were further correlated by themselves to give rise to autocorrelations $R_{pp}(\tau)$. Although autocorrelations are commonly plotted with the time delay τ on the abscissa, the present data are plotted against a normalized "convection distance" $\bar{D}_c = \tau U_c/\delta_0$ to facilitate the discussion, where a value of $U_c \approx 0.65 U_\infty \approx 810 \text{ ms}^{-1}$ (2650 ft/s) was used. Thus, both U_c and δ_0 were assumed constant, although they were expected to increase through the expansions. The increase of both terms would approximately be compensated by the normalization. It may be noted that using \bar{D}_c tacitly accepted Taylor's hypothesis, \bar{D}_c representing the dis-

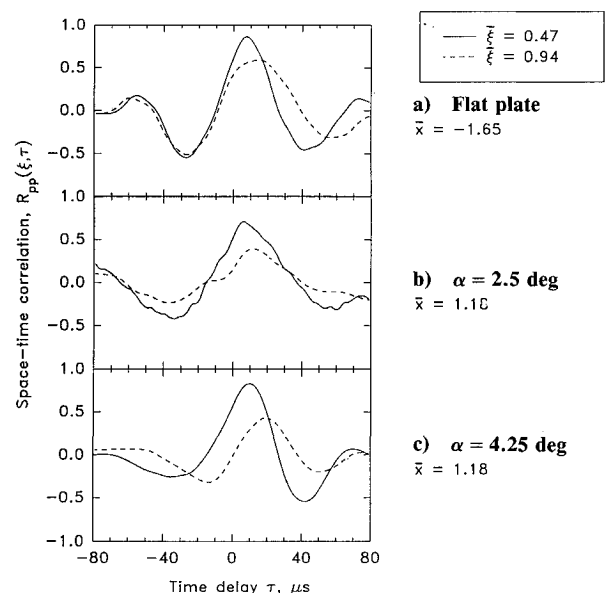


Fig. 7 Space-time correlations of surface pressure fluctuations past expansion corners.

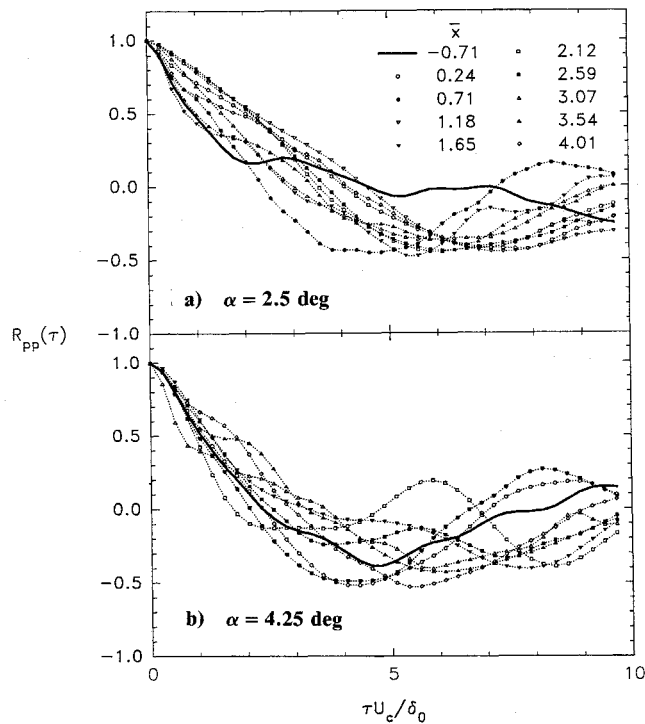


Fig. 8 Autocorrelations of surface pressure fluctuations past expansion corners.

tance in terms of δ_0 that a disturbance is convected at a velocity U_c . The autocorrelations of the surface pressure fluctuations $R_{pp}(\tau)$ are plotted in Fig. 8 for both corner angles. In the figures, the autocorrelation upstream of the corner is shown as a thick solid line, whereas the autocorrelations downstream are shown as symbols connected by dotted lines. The symbols denote only one-quarter of the total data for each correlation to avoid cluttering the plots. Also, the legend for Fig. 8b is the same as that for Fig. 8a and is omitted for clarity.

The autocorrelations showed shapes typical of those encountered in surface pressure measurements at lower Mach numbers, namely, they exhibited a rapid decrease followed by a shallow negative lobe and a subsequent shallow positive lobe. For larger values of \bar{D}_c , the shallow positive lobe in $R_{pp}(\tau)$ in the present experiments might be affected by disturbances from flow starting or stopping because of the short duration of the quasisteady test period. It was difficult to detect any trends in the autocorrelations, and it was thought there may not be any distinct trends in the shape of the autocorrelations downstream due to the weak expansions encountered.

An integral scale and a microscale were estimated from the autocorrelations. These estimates were of the ensemble of the downstream measurements for each test configuration. The determination was affected by "jitters" and "bumps" in the curves. The integral scale, found by integrating the autocorrelations, was estimated to be about $4.5\delta_0$ for the 2.5-deg expansion and about $6.7\delta_0$ for the 4.25-deg expansion, with an rms scatter of ± 20 and $\pm 10\%$. (In physical dimensions, the integral scales were 75 ± 15 and $110 \pm 10 \mu\text{s}$, respectively.) The integral scale obtained was larger than the incoming boundary-layer thickness, a phenomenon also found in previous flat-plate studies that was attributed by Dolling and Dussauge²⁴ to the limited data bandwidth. Despite the difficulties associated with data bandwidth, the integral scale is a rough measure of the interval that a turbulent signal is correlated with itself, and the trend of the data indicated that the "large-scale" surface pressure fluctuations maintained their identities longer for the stronger expansion.

The microscale determination was also affected by the "jaggedness" of the autocorrelations, perhaps more so than

Table 1 Test conditions

| | | |
|------------|-----------------------------------|-------------------------------|
| M_∞ | 8 | |
| U_∞ | 1.24 km s ⁻¹ | (4080 ft/s) |
| p_0 | 5.38 MPa | (780 psia) |
| T_0 | 820 K | (1480°R) |
| Re | $10.2 \times 10^6 \text{ m}^{-1}$ | $(3.1 \times 10^6/\text{ft})$ |
| p_∞ | 0.55 kPa | (0.08 psia) |
| T_∞ | 59 K | (107°R) |

for the integral scale, and the following technique was used to estimate the microscale. Only data very near the origin were fitted to an osculating parabola, with data thresholds of $\tau U_c/\delta_0 = \pm 2, \pm 1, \pm 0.75, \pm 0.5$, and ± 0.25 . A second-order least-squares fit was then performed on the microscales obtained from the data within the five individual thresholds. Extrapolation to $\tau U_c/\delta_0 = 0$ of the curvefit constants obtained for the data thresholds then gave the desired value of the microscale. The composite value of the microscale for both expansion corners given by the previous technique was about $\tau U_c/\delta_0 = 1$, with an rms scatter of 20–40%. This value was also on the same order as that found for the upstream flow. In physical dimensions, this corresponded to a time of $16 \mu\text{s}$ and, invoking Taylor's hypothesis, a distance of about one boundary-layer thickness. The present estimates were much lower than those of Raman.²⁷ In Raman's experiments at Mach 7.4, the flow past a flat plate at Reynolds numbers of $Re_x = 0.93$ and 1.34×10^6 produced boundary layers 17.5 mm (0.67 in.) and 14.5 mm (0.57 in.) thick, respectively. For both flows, the microscale was about $50 \mu\text{s}$. The present estimates were thought to be more accurate than Raman's since only data very near the origin were fitted to the osculating parabola by a limiting process.

Conclusions

The surface pressure fluctuations of hypersonic turbulent flow downstream of small expansion corners were found to be normally distributed through the expansion process but were severely attenuated. The pressure fluctuations indicated that there was no recovery to an equilibrium turbulent flow within four to six incoming boundary-layer thicknesses downstream even though the mean pressures reached downstream inviscid values within that distance. The fluctuations were convected with a velocity comparable to that on a flat plate, and these fluctuations maintained their identities longer for stronger expansions. The extremely large damping of the pressure fluctuations, even by small corner angles, may be exploited in fatigue design.

Acknowledgments

The research reported was supported by NASA Langley Grant NAG 1-891 monitored by J. P. Weidner. This support is gratefully acknowledged. The authors thank E. G. Pace and J. M. Dodson II for assisting with the experiments and Gene Sloan and Jim Holland for fabricating parts of the model. The authors enjoyed useful discussions with Xue-Ying Deng of the Beijing University of Aeronautics and Astronautics on relaminarization and retransition.

References

- ¹Dussauge, J. P., and Gaviglio, J., "The Rapid Expansion of a Supersonic Turbulent Flow: Role of Bulk Dilatation," *Journal of Fluid Mechanics*, Vol. 174, Jan. 1987, pp. 81–112.
- ²Smith, D. R., and Smits, A. J., "The Rapid Expansion of a Turbulent Boundary Layer in a Supersonic Flow," *Theoretical and Computational Fluid Dynamics*, Vol. 2, 1990, pp. 319–328.
- ³Goldfeld, M. A., and Tyutina, E. G., "Relaminarizatsiya sverkhzvukovogo turbulentnogo pogrannichnogo sloya pri bistro-rasshirenii okolo uglovoy točki," Inst. of Theoretical and Applied Mechanics, Siberian Division of the USSR Academy of Sciences, Preprint No. 12-82, Novosibirsk, Russia, 1982.
- ⁴Goldfeld, M. A., "On the Reverse Transition of Compressible Turbulent Boundary Layer in a Transverse Flow Around a Convex Corner Configuration," *Proceedings of the IUTAM Symposium on*

Laminar-Turbulent Transition, edited by V. V. Kozlov, Springer-Verlag, Berlin, Germany, 1985, pp. 515-520.

⁵Narasimha, R., and Viswanath, P. R., "Reverse Transition at an Expansion Corner in Supersonic Flow," *AIAA Journal*, Vol. 13, No. 5, 1975, pp. 693-695.

⁶Lu, F. K., and Chung, K.-M., "Downstream Influence Scaling of Turbulent Flow Past Expansion Corners," *AIAA Journal*, Vol. 30, No. 12, 1992, pp. 2976, 2977.

⁷Stollery, J. L., and Bates, L., "Turbulent Hypersonic Viscous Interaction," *Journal of Fluid Mechanics*, Vol. 63, Pt. 1, March 1974, pp. 145-156.

⁸Laganelli, A. L., Martellucci, A., and Shaw, L. L., "Wall Pressure Fluctuations in Attached Boundary-Layer Flow," *AIAA Journal*, Vol. 21, No. 4, 1983, pp. 495-502.

⁹Lu, F. K., "Initial Operation of the UTA Shock Tunnel," AIAA Paper 92-0331, Jan. 1992.

¹⁰Minucci, M. A. S., and Nagamatsu, H. T., "An Investigation of Hypersonic Shock Tunnel Testing at an Equilibrium Interface Condition at 4100 K: Theory and Experiment," AIAA Paper 91-1707, June 1991.

¹¹Arrington, J. P., Joiner, R. C., Jr., and Henderson, A., Jr., "Longitudinal Characteristics of Several Configurations at Hypersonic Mach Numbers in Conical and Contoured Nozzles," NASA TN D-2489, Sept. 1964.

¹²Elfstrom, G. M., "Turbulent Hypersonic Flow at a Wedge-Compression Corner," *Journal of Fluid Mechanics*, Vol. 53, Pt. 1, May 1972, pp. 113-127.

¹³Chew, Y. T., "Shockwave and Boundary Layer Interaction in the Presence of an Expansion Corner," *Aeronautical Quarterly*, Vol. 30, Aug. 1979, pp. 506-527.

¹⁴Bloy, A. W., "The Expansion of a Hypersonic Turbulent Boundary Layer at a Sharp Corner," *Journal of Fluid Mechanics*, Vol. 67, Pt. IV, Feb. 1975, pp. 647-655.

¹⁵Daum, F. L., and Gyarmathy, G., "Condensation of Air and Nitrogen in Hypersonic Wind Tunnels," *AIAA Journal*, Vol. 6, No. 3, 1968, pp. 458-465.

¹⁶Bradshaw, P., "An Improved Van Driest Skin-Friction Formula for Compressible Turbulent Boundary Layers," *AIAA Journal*, Vol. 15, No. 2, 1977, pp. 212-214.

¹⁷Chung, K.-M., and Lu, F. K., "An Experimental Study of a Cold-Wall Hypersonic Boundary Layer," AIAA Paper 92-0312, Jan. 1992.

¹⁸Chung, K.-M., "Shock Impingement Near Mild Hypersonic Expansion Corners," Ph.D. Dissertation, Univ. of Texas at Arlington, Arlington, TX, Dec. 1992.

¹⁹van Driest, E. R., "The Problem of Aerodynamic Heating," *Aeronautical Engineering Review*, Vol. 15, No. 10, 1956, pp. 26-41.

²⁰Sun, C. C., and Childs, M., "A Wall-Wake Velocity Profile for Compressible Nonadiabatic Flows," *AIAA Journal*, Vol. 14, No. 6, 1976, pp. 820-822.

²¹Davies, W. R., and Bernstein, L., "Heat Transfer and Transition to Turbulence in the Shock-Induced Boundary Layer on a Semi-Infinite Flat Plate," *Journal of Fluid Mechanics*, Vol. 36, Pt. 1, March 1969, pp. 87-112.

²²Schewe, G., "On the Structure and Resolution of Wall-Pressure Fluctuations Associated with Turbulent Boundary-Layer Flows," *Journal of Fluid Mechanics*, Vol. 134, Sept. 1983, pp. 311-328.

²³Gibson, B., and Dolling, D. S., "Wall Pressure Fluctuations Near Separation in a Mach 5, Sharp Fin-Induced Turbulent Interaction," AIAA Paper 91-0646, Jan. 1991.

²⁴Dolling, D. S., and Dussauge, J. P., "Fluctuating Wall-Pressure Measurements," *A Survey of Measurements and Measuring Techniques in Rapidly Distorted Compressible Turbulent Boundary Layers*, edited by H. H. Fernholz, P. J. Finley, J. P. Dussauge, and A. J. Smits, AGARD-AG-315, 1988, Chap. 8.

²⁵Bendat, J. S., and Piersol, A. G., *Random Data*, 2nd ed., Wiley, New York, 1986, Chaps. 3, 5.

²⁶Narasimha, R., and Sreenivasan K. R., "Relaminarization of Fluid Flows," *Advances in Applied Mechanics*, Vol. 19, 1979, pp. 221-309.

²⁷Raman, K. R., "Surface Pressure Fluctuations in Hypersonic Turbulent Boundary Layers," NASA CR-2386, Feb. 1974.